한국공작기계학회논문집 Vol.18 No.1 2009. 2. pp. 90~102
Transactions of the Korean Society of Machine Tool Engineers

Nonlinear Friction Control Using the Robust Friction State Observer and Recurrent Fuzzy Neural Network Estimator

Seong Ik Han*

(논문접수일 2008. 8. 19, 심사완료일 2009. 1. 19)

강인한 마찰 상태 관측기와 순환형 퍼지신경망 관측기를 이용한 비선형 마찰제어

한성익*

Abstract

In this paper, a tracking control problem for a mechanical servo system with nonlinear dynamic friction is treated. The nonlinear friction model contains directly immeasurable friction state and the uncertainty caused by incomplete modeling and variations of its parameter. In order to provide the efficient solution to these control problems, we propose a hybrid control scheme, which consists of a robust friction state observer, a RFNN estimator and an approximation error estimator with sliding mode control. A sliding mode controller and a robust friction state observer is firstly designed to estimate the unknown internal state of the LuGre friction model. Next, a RFNN estimator is introduced to approximate the unknown lumped friction uncertainty. Finally, an adaptive approximation error estimator is designed to compensate the approximation error of the RFNN estimator. Some simulations and experiments on the mechanical servo system composed of ball-screw and DC servo motor are presented. Results demonstrate the remarkable performance of the proposed control scheme.

Key Words : LuGre friction model(LuGre 마찰모델), Sliding mode control(슬라이딩 모드제어), Robust friction state observer(강인마찰상태관측기), Recurrent fuzzy neural networks(순환형 퍼지신경망), Estimation error estimator(추정오차 추정기)

1. Introduction

A nonlinear friction is an unavoidable phenomenon appeared in mechanical system between two contact surfaces. This often worsens the performance of the servo control system since it causes the steady state error, limit

* Dept. of Electrical Automation, Suncheon First College (hansng@suncheon.ac.kr)
Address: 540-744 9-3 Dukwoldong, Suncheon, Chennam, Korea

cycle and low bandwidth in closed-loop control system. Specially, in the low velocity range the effects of the friction on the performance of the servo system are more greater than moderate velocity range since the friction forces/torques coming from the stick and pre-sliding motion are dominant than control input forces/torques. The friction model at moderate velocity, called as the classical friction model is built by the Coulomb and viscous friction. However, this classical friction model cannot capture the characteristics such as the Stribeck effect, stick-slip, pre-sliding hysteretic motion, break-away force, which play a significant role in application on high precise motion control.

Canudas de Wit et al.[1], presented a dynamic friction model, called as LuGre friction model, which captures both dynamic friction of low velocity and steady state friction characteristic. As the LuGre friction model has the simple and nice structure mathematically, then many researchers have chosen it as a representative friction model to control the frictional servo mechanical system such as the robots, X-Y table, electro-mechanical actuator, tire/road friction and machine tools, etc. But since the LuGre friction model has some problem in describing the hysteresis motion in pre-sliding, Dupont et al.[2] developed the improved friction model, called 'elasto-plastic model'. Moreover, Swevers et al.[3,4] and Han et al.[5] developed the improved friction model, called 'Leuven model' and 'Maxwell-slip model', respectively, where the hysteresis property in pres-sliding range is modified, using the Preisach technique frequently used in magnetism[6]. However, this model has not been widely used yet due to the complexity of modeling the hysteresis phenomenon in the pre-sliding range. Therefore, several researches[7~9] have adopted to control the friction system as the LuGre model since it almost satisfy the most part of the nonlinear friction characteristic except the hysteresis micro unit motion of the pre-sliding range and is easier to analyze and implement than other second-order friction models.

In general, the control scheme on the compensation of nonlinear friction is divided into two sides of approaches: friction model-based and nonmodel-based one. The latter approach is mainly used when the exact friction model cannot be constructed and no need precise tracking performance. The neural network[10] and variable structure control[11] correspond to this case. While the model-based method[12,13] can be applied to the case that the identification of the parameter of friction is possible with in a certain range of a precision degree, and so a more precise tracking performance can be obtained. However, this approach may give a little complexity and difficulty of the exact identification of friction parameters to the control system. Moreover, since the state representing the bristle deformations of the LuGre friction model cannot be measured directly, the estimation process for it must be presented to obtain more precise information on the friction dynamic. In addition, the parameter variations and unmodeled disturbances can reduce the performance of the control system due to the model-based property of the control system. Thus, the robust controller to overcome the modeling error and parameter variations must be designed to obtain the precise tracking performance. The approximation on the uncertainties of the system can be done well by the fuzzy or neural networks scheme.

Recently, fuzzy logic and neural networks much research has been much attention in identification and control of complex dynamic systems. They have both capability of approximating any continuous nonlinear functions closely[14], but there are some differences between them. The fuzzy logic possesses linguistic information and logic control and the neural networks have the learning, parallelism, and fault-tolerance. Moreover, the development of integrated fuzzy neural networks (FNN), which combine the capability of both of their advantages, has also grown[15~17]. However, the draw back of the FNN is that the application domain is limited to static mapping due to its feedforward network structure which requires a large number of neuron or membership function and is sensitive to the training data. On the other hand, the recurrent FNN (RFNN)[18~20] naturally involves dynamic elements in the form of feedback connections used as internal memories. Thus, the RFNN is a dynamic mapping and demonstrates good control performance in the presence of uncertainty such as parameter variations of the system, external load, unmodeled dynamics compared to the feedforward FNN.

In this paper, we propose a hybrid friction control system comprised of a sliding mode controller, a robust dynamic friction state observer, a RFNN and an approximation error estimator. A friction state observer can estimate the immeasurable internal friction state of the LuGre friction model. In addition, a RFNN is introduced to approximate the uncertainty and the adaptive robust estimator for the approximation error is also designed. A mechanical servo system composed of ball-screw and DC servo motor is chosen to demonstrate the good performance of a proposed control scheme through the simulation and experiment.

2. SMC control and Robust Friction State Observer

2.1 System dynamics

The dynamic model for the mechanical system in the presence of friction is

$$J\ddot{q} + \sigma_2\dot{q} + T_f = u \tag{1}$$

where J is a moment of inertia, σ_2 is a viscous friction coefficient, T_f is a nonlinear dynamic friction. In well-known LuGre friction model, the interface between two surfaces is modeled by contact between sets of elastic bristles shown in Fig. 1. When a tangential torque is applied, the elastic bristle will deflect like spring that gives rise to the friction torque. If the torque is increased beyond a certain magnitude, some of the elastic bristles deflect so much and they will slip. An average defection of the elastic bristle is defined by z and its dynamic is

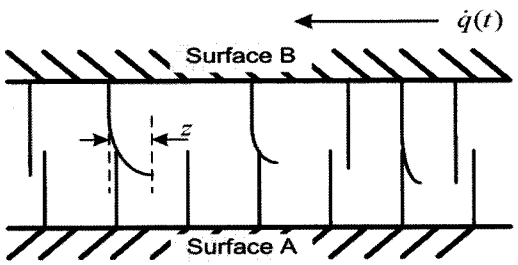

Fig. 1 The friction interfaces with bristles between two surfaces

given as follows[1]:

$$\dot{z} = \dot{q} - f(\dot{q})z \tag{2}$$

where

$$f(\dot{q}) = \frac{|\dot{q}|}{g(\dot{q})} \tag{3}$$

In Eq. (2), $\dot{q}$ is the relative velocity between two contact surfaces. The function $g(\dot{q})$ is positive and depends on many factors such as the material properties, lubrication, and temperature. The function $g(\dot{q})$ is parameterized as follows:

$$\sigma_0 g(\dot{q}) = T_c + (T_s - T_c)e^{-(\dot{q}/\dot{q}_s)^i} \tag{4}$$

where T_c is Coulomb friction, T_s is stiction level, $\dot{q}_s$ is Stribeck velocity and i denotes coefficient depending on the friction system, where i is selected as 2 in metal friction and 0.5 in tire/road friction system, respectively. The dynamic friction term excluding viscous friction torque is described by

$$T_f = \sigma_0 z + \sigma_1\dot{z} \tag{5}$$

where σ_0 is the stiffness of the elastic bristle, σ_1 is a damping coefficient in elastic range. In Eq. (2) and Eq. (5), T_f can be rewritten by

$$T_f = \Phi(\dot{q})z + \sigma_1\dot{q} \tag{6}$$

where the auxiliary function $\Phi(\dot{q})$ is defined as follows:

$$\Phi(\dot{q}) = \sigma_0 - \sigma_1 f(\dot{q}) \tag{7}$$

Let us introduce Eq. (6) into Eq. (1) and consider the uncertainty of the modeling error of the friction and other disturbances.

$$J\ddot{q} + \sigma_3\dot{q} + T_z = u \tag{8}$$

where $\sigma_3 = \sigma_1 + \sigma_2$ and $T_z = \Phi(\dot{q})z$.

2.2 Design of sliding mode controller and friction state observer

We define the sliding surface of the SMC of the integral type and the position tracking error $e(t)$ as follows:

$$s = \dot{e} + c_1 e + c_2 \int e dt \tag{9}$$

$$e = q_d - q \tag{10}$$

where c_1 and c_2 are the positive design constants and q_d is the desired position trajectory. Our objective is to choose control input u such that the system state is driven to the sliding surface $s = 0$ regardless of the friction. The control input can be adopted by the form with unified smooth control law as follows:

$$u = J(c_1 \dot{e} + \ddot{q}_d + c_2 e) + \sigma_3 \dot{q} + \beta s + T_z \tag{11}$$

where β is a positive constant. Let us introduce Eq. (11) into Eq. (8) and rearrange it in terms of tracking error as follows:

$$J[(\ddot{q}_d - \ddot{q}) + c_1 \dot{e} + c_2 e] = -\beta s \tag{12}$$

In Eq. (12), the following closed-loop error is obtained as

$$\dot{s} = -\frac{1}{J}\beta s \tag{13}$$

Define the Lyapunov function as the following non-negative function:

$$V_1 = \frac{1}{2} J s^2 \tag{14}$$

Taking the time derivative of Eq. (14) and considering Eq. (13), the following result can be obtained as follows:

$$\dot{V}_1 = J s \dot{s} = -\beta s^2 \le 0 \tag{15}$$

From the above equation, $W_1(Z(t))$ is defined by

$$W_1(Z(t)) = \beta s^2 \le -\dot{V}_1 \tag{16}$$

Since $\dot{V}_1 \le 0$, V_1 is nonincreasing. Thus, it has a limit $V_{1\infty}$ as $t \to \infty$. Integrating Eq. (16), then

$$\lim_{t\to\infty} \int_{t_0}^{t} W_1(Z(\tau)) d\tau \le -\lim_{t\to\infty} \int_{t_0}^{t} \dot{V}_1 d\tau$$
$$= \lim_{t\to\infty} \{V_1(Z(t_0)) - V_1(Z(t))\} = V_1(t_0) - V_1(\infty) \tag{17}$$

which means that $\int_{t_0}^{t} W_1(Z(\tau)) d\tau$ exits and finite. Since $W_1(Z(t))$ is also uniformly continuous, the following result can be obtained from Barbalat lemma[21]:

$$\lim_{t\to\infty} \int_{t_0}^{t} W_1(Z(\tau)) d\tau < \infty \tag{18}$$

Also, $\dot{W}_1(t)$ is bounded, so by Barbalat lemma, $\lim_{t\to\infty} W_1(t) = 0$. That is, $s \to 0$ as $t \to \infty$, and the SMC control system can have the asymptotic stability.

2.3 Design uncertainty estimator using recurrent fuzzy neural network

However, since the friction state z cannot be measured directly and the friction parameters can be changed according to the contact surface condition and other variation of lubrication property, the friction function T_z of the control input of Eq. (11) cannot be known. Furthermore, since the exact measurements of each friction parameter can be very hard to be accomplished, the discrepancy between real friction model and identified one cannot be avoidable. Thus, the controller based on the fixed friction parameters has naturally a weakness to the variation of friction parameters and in complete parameter modeling. Therefore, the friction state observer and uncertainty estimator of friction parameters must be adopted to design the robust controller. The dynamics of Eq. (8) containing the uncertainty can be changed as

$$J\ddot{q} + \sigma_3 \dot{q} + T_z + T_d = u \tag{19}$$

where T_d is the total lumped friction uncertainty.

Now, since the value of T_d cannot be known exactly, the recurrent fuzzy neural network based estimator is adopted to approximate the value of T_d. Then, the control input of Eq. (11) is rewritten as

$$u_{RFNN} = J(c_1 \dot{e} + \ddot{q}_d + c_2 e) + \sigma_3 \dot{q} + \beta s + \hat{T}_z + \hat{T}_d \tag{20}$$

where $\hat{T}_d$ is estimate of T_d and $\hat{T}_z = \Phi(\dot{q})\hat{z}$, where $\hat{z}$ is the estimate of z which can be obtained from the friction state observer to be presented in next section.

A four-layer recurrent fuzzy neural network[18] is shown in Fig. 2. Layer *I* is the input layer, which accepts the two input variables. In layer *II* representing the fuzzy rules, Gaussian membership values are calculated. The link before layer *III* represents the preconditions of the rules, and the links after layer *III* represent the consequence of the rule nodes. Layer *IV* is the output layer.

The interactions for the layers are given as follows:

A. Description of the RFNN

Layer I (Input layer): For every node i in this layer, the net input and the net output are represented as

$$\text{net}_i^I = u_i^I + w_i^I \cdot O_i^I(N-1) \tag{21}$$

$$O_i^I(N) = f_i^I(\text{net}_i^I)) = \text{net}_i^I(N),\ i = 1,2 \tag{22}$$

where $u_1^1 = e$, $u_2^1 = \dot{e}$, w_i^I is the recurrent weights for the units in the input space and N denotes the number of iterations.

Layer II (Membership layer): In this layer, each node performs a membership function. The Gaussian function is adopted as the membership function. For the jth node,

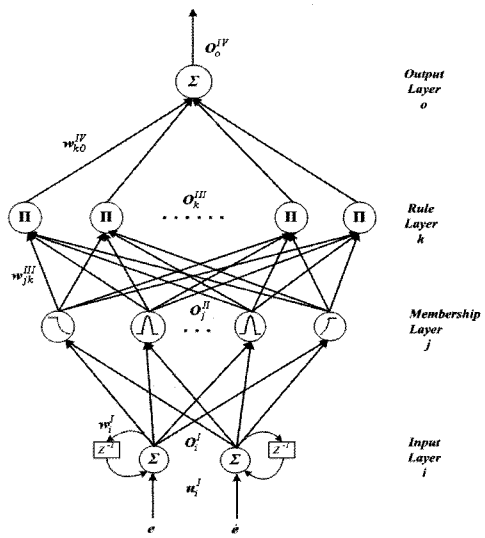

Fig. 2 Structure of the four-layer RFNN

$$\text{net}_j^{II}(N) = -\frac{(u_i^{II} - m_{ij})^2}{(\sigma_{ij})} \tag{23}$$

$$O_j^{II}(N) = f_j^{II}(\text{net}_j^{II}(N)) = \exp(\text{net}_j^{II}(N)),\ j = 1,\ldots,n \tag{24}$$

where m_{ij} and σ_{ij} are, respectively, the mean and the standard deviation of the Gaussian function in the jth term of the ith input linguistic variable u_i^{II} to the node of layer *II*, and n is the total number of the linguistic variables with respect to the input nodes.

Layer III (Rulelayer): Each node k in this layer is denoted by *II*, which multiplies the input signals and outputs the result of the product. For the kth rule node

$$\text{net}_k^{III}(N) = \prod_j w_{jk}^{III} u_j^{III}(N) \tag{25}$$

$$O_k^{III}(N) = f_k^{III}(\text{net}_k^{III}(N)) = \text{net}_k^{III}(N), k = 1, \ldots, l \tag{26}$$

where u_j^{III} represents the jth input to the node of layer *III*, w_{jk}^{III} is the weights between the membership layer and the rule layer, are assumed to be unity; l is the number of rules with complete rule connection if each input node has the same linguistic variables.

Layer IV (Output layer): The single node o in this layer is labeled as Σ, which computes the overall output as the summation of all input signals:

$$\text{net}_o^{IV}(N) = \sum_k w_{ko}^{IV} u_k^{IV}(N) \tag{27}$$

$$O_o^{IV}(N) = f_o^{IV}(\text{net}_o^{IV}(N)) = \text{net}_o^{IV}(N),\ o = 1 \tag{28}$$

where the connecting weight w_{ko}^{IV} is the output action strength of the oth output associated with the kth rule, u_k^{IV} represents the kth input to the node of layer *IV*, and O_o^{IV} is the output of the fuzzy neural network.

B. On-line learning algorithm

In order to train the RFNN according to the minimization of the error using the gradient search algorithm, the e and $\dot{e}$ are taken as the inputs of the RFNN and the energy function is defined as

$$E = \frac{1}{2}e^2 \tag{29}$$

According to the gradient descent method, the detail explanations on the update of the weights and mean and standard deviation of the hidden layer in each layer are illustrated in reference[20] and from[20], the updates are given as follows:

$$w_i^I(N+1) = w_i^I(N) + \Delta w_i^I \tag{30}$$

$$m_{ij}(N+1) = m_{ij}(N) + \Delta m_{ij} \tag{31}$$

$$\sigma_{ij}(N+1) = \sigma_{ij}(N) + \Delta \sigma_{ij} \tag{32}$$

$$w_{ko}^{IV}(N+1) = w_{ko}^{IV}(N) + \Delta w_{ko}^{IV} \tag{33}$$

2.4 Design the robust sliding mode controller

From the RFNN, the approximation of uncertainty $\hat{T}_d$ can be obtained. However, since the exact estimation of the uncertainty is hard to be obtained from the RFNN estimator, the following RFNN control input with robust term (RFNR) is proposed to consider the approximation error as follows:

$$u_{RFNR} = J(c_1\dot{e} + \ddot{q}_d + c_2 e) + \sigma_3\dot{q} + \beta s + \hat{T}_z + \hat{T}_d + \hat{U} \tag{34}$$

where $\hat{U}$ is estimate of uncertainty estimation error $U(= T_d - \hat{T}_d)$. Let us introduce Eq. (34) into Eq. (19) and rearrange it in terms of tracking error as follows:

$$\begin{aligned} J[(\ddot{q}_d - \ddot{q}) + c_1\dot{e} + c_2 e] &= T_z - \hat{T}_z - \beta s + U - \hat{U} \\ &= \Phi(\dot{q})\tilde{z} - \beta s + \tilde{U} \end{aligned} \tag{35}$$

where $\tilde{U} = U - \hat{U}$. Eq. (35) can be written by

$$\dot{s} = \frac{1}{J}(\Phi(\dot{q})\tilde{z} - \beta s + \tilde{U}) \tag{36}$$

As an extension of author's previous research[13], a robust friction state observer, which exponentially estimates the state z, is given by

$$\hat{z} = w + \frac{J}{\sigma_1}s + k_1 e \tag{37}$$

$$\begin{aligned} \dot{w} = \frac{1}{\sigma_1}[&-\sigma_0 w - \sigma_2\dot{q} - J\frac{\sigma_0}{\sigma_1}s + u_{RFNR} + \Phi(\dot{q})s \\ &- \sigma_0 k_1 e - J(\ddot{q}_d + c_1\dot{e} + c_2 e) - \hat{T}_d - \hat{U}] - k_1\dot{e} \end{aligned} \tag{38}$$

where w is auxiliary variable and k_1 takes a role of the adjusting transient performance of the observer. Let us define the Lyapunov function as follows:

$$V_2 = V_1 + \frac{1}{2}\sigma_1\tilde{z}^2 + \frac{1}{2\eta}\tilde{U}^2 \tag{39}$$

The time derivative of Eq. (39) is

$$\begin{aligned} \dot{V}_2 &= s[\Phi(\dot{q})\tilde{z} - \beta s + \tilde{U}] + \sigma_1\tilde{z}\dot{\tilde{z}} + \frac{1}{\eta}\tilde{U}\dot{\tilde{U}} \\ &= s[\Phi(\dot{q})\tilde{z} - \beta s + \tilde{U}] + \sigma_1\tilde{z}(\dot{z} + \dot{\hat{z}}) + \frac{1}{\eta}\tilde{U}(-\dot{\hat{U}}) \\ &= s[\Phi(\dot{q})\tilde{z} - \beta s + \tilde{U}] \\ &\quad + \sigma_1\tilde{z}\left[\dot{q}(t) - f(\dot{q})z(t) + \dot{w} + \frac{J}{\sigma_1}\dot{s} + k_1\dot{e}\right] + \frac{1}{\eta}\tilde{U}(-\dot{\hat{U}}) \\ &= -\beta s^2 - \sigma_0\tilde{z}^2 - \tilde{z}\tilde{U} + \tilde{U}(s - \frac{1}{\eta}\dot{\hat{U}}) \end{aligned} \tag{40}$$

The adaptive robust estimation law for the estimate of uncertainty approximation error is chosen by

$$\dot{\hat{U}} = \eta \cdot s \tag{41}$$

Then, Eq. (40) can be written as

$$\begin{aligned} \dot{V}_2 &= -\beta s^2 - \sigma_0\tilde{z}^2 - \tilde{z}\tilde{U} \\ &\le -\sigma_0\tilde{z}^2 - \tilde{z}\tilde{U} = -\boldsymbol{Z}^T\boldsymbol{M}\boldsymbol{Z} \le 0 \end{aligned} \tag{42}$$

where $Z = [\tilde{z} \quad \tilde{U}]^T$ and $M = \begin{bmatrix} \sigma_0 & 1 \\ 0 & 0 \end{bmatrix}$. Since the matrix M is the positive semi-definite, Eq. (42) is negative semi-definite. From the above equation, define $W_2(Z(\tau))$

$$W_2(Z(\tau)) = \sigma_0\tilde{z}^2 + \tilde{z}\tilde{U} \le -\dot{V}_2 \tag{44}$$

Then, $\lim_{t\to\infty} W_2(t) = 0$ by Barbalat lemma[21]. That is, $s \to 0$, $\tilde{z} \to 0$ and $\tilde{U} \to 0$ as $t \to \infty$. Therefore, the SMC control system that considers the unknown friction uncertainty and the approximation error can have the asymptotic stability and good robustness to the disturbance. The schematic diagram of the proposed control system is depicted in Fig. 3.

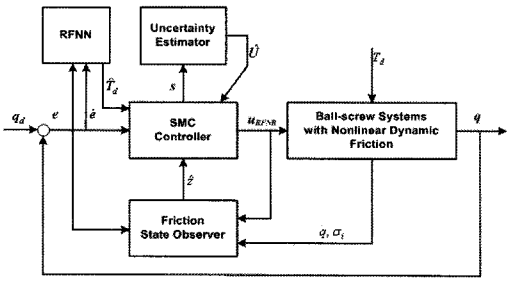

Fig. 3 Schematic diagram of the proposed control system

3. Results of Simulation and Experiment

The simulation and experiment are executed for the verification of the precision tracking control of a mechanical servo system, which is composed of ball-screw and DC servo motor as shown in Fig. 4. A schematic diagram and photograph the mechanical servo system are depicted in Fig. 4 and Fig. 5, respectively. The identified system parameters through experiments are given in Table 1 and the specifications of the system components are also given in Table 2. The identification process of the dynamic friction parameters is omitted in this paper. The radian position of the mechanical servo system is obtained by the precise encoder coupled with the DC motor shaft.

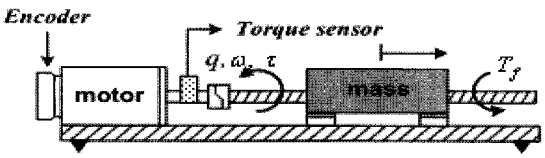

Fig. 4 Schematic diagram of the mechanical servo system

Fig. 5 Photograph of the mechanical servo control system

3.1 Results of simulation

To investigate the effectiveness the proposed control system, three control schemes are designed; a sliding mode controller (SMC), a sliding mode controller with friction state observer (SOB) and a sliding mode controller using RFNN and friction state observer with adaptive robust estimator (SOB+RFNR). Moreover, the following

Table 1 Parameters of ball-screw and friction model

Symbol	Value
J	*0.246 kgm²*
T_c	*0.088 Nm*
T_s	*0.11 Nm*
$\dot{q}_s$	*0.056 rad/sec*
σ_0	*86.4 Nm/rad*
σ_1	*4.7 Nmsec/rad*
torque constant	*0.3 Nm/A*
amplifier gain	*2.72 A/V*

Table 2 Specification of system components of the control system

Item	Specification
IBM PC	Pentium II, MS-DOS, C-language
Data Acquisition board	DR8330, DA resolution : 12 bits
Encoder counter board	PCL-833Resolution : 32bits
Motor driver	FDD-106PD
DC servo motor	300W, 3000rpm
Encoder	ITD 21 B14, resolution 10000 pulse/rev
Ball-screw	THK, C0 grade

cases are tested in the simulation including nominal case 1 ($\overline{T_i}, \overline{\sigma_i}$), and friction parameter variation case 2:

Case 1: $T_i = \overline{T_i}$, $i = c, s$ and $\sigma_i = \overline{\sigma_i}$, $i = 0,1,2,3$

Case 2: $T_i = 2 \times \overline{T_i}$, $i = c, s$ and $\sigma_i = 2 \times \overline{\sigma_i}$, $i = 0,1,2,3$

The simulation is carried out using the 'Matlab' package. $q_d = 0.2 \times \exp(2\pi \times 0.3t) \times \sin(2\pi \times 0.05t)$ is chosen as a command input in the simulation. The

RFNN has two, five, five, and one neuron at the input, membership, rule and output layers, respectively. The Gaussian function and the connecting weights are initialized with the maximum value of each input and the random number via some trials in order to prevent the divergence of their outputs.

First, for case 1, Fig. 6 shows the tracking response when SMC is applied to the mechanical servo system with normal friction model. It can be shown that the position tracking performance is very poor since the friction disturbs the position performance in low velocity and low control torque. Fig. 7 and 8 show the tracking responses of the SOB and SOB+RFNR control system where the tracking performances are significantly improved than the previous result under the same controller parameters as the SMC control system. This reason is that the friction state observer compensates the friction torque in low level of the position ranges as shown in Fig. 8 and 10. Therefore, it is proven that the proposed friction state observer can estimate the unknown friction state very well. The tracking errors of the SOB and SOB+RFNR

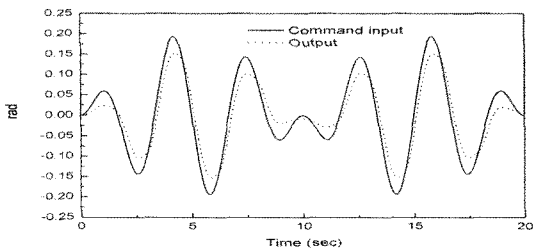

Fig. 6 Simulated results of the SMC control system: tracking

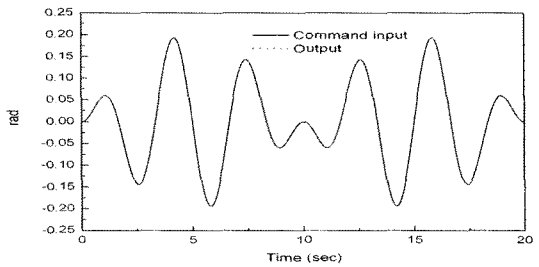

Fig. 7 Simulated results of the SOB control system for the nominal system: tracking responses

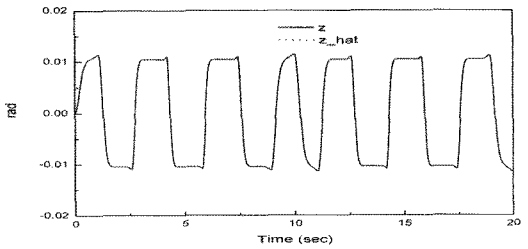

Fig. 8 Simulated results of the SOB control system for the nominal system: z and $\hat{z}$

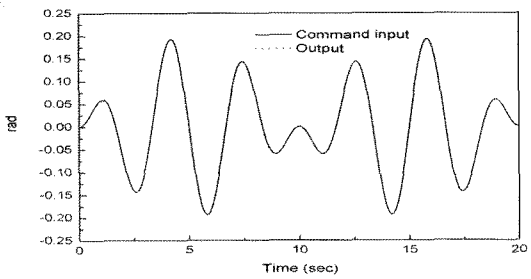

Fig. 9 Simulated results of the SOB+RFNR control system for the nominal system: tracking responses

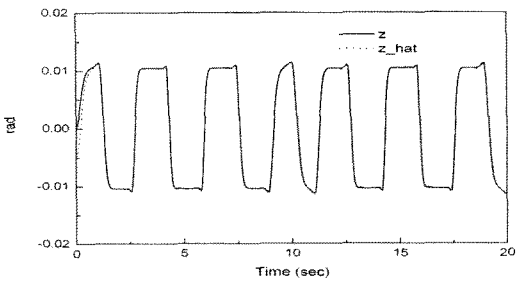

Fig. 10 Simulated results of the SOB+RFNR control system for the nominal system: z and $\hat{z}$

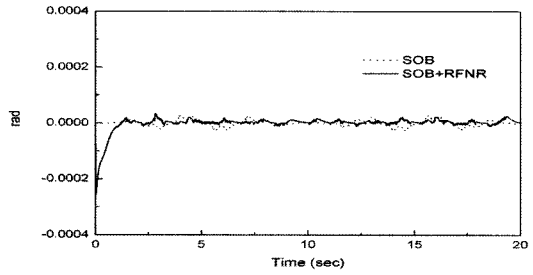

Fig. 11 Simulated results of the SOB+RFNR control system for the nominal system: tracking errors

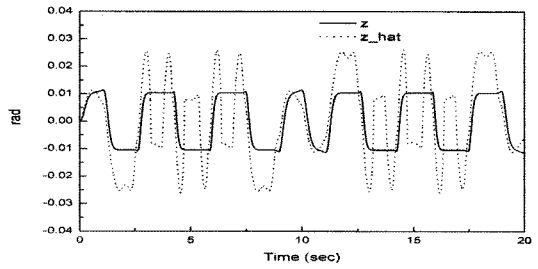

Fig. 12 Simulated results of the SOB control system for the disturbed system: z and $\hat{z}$

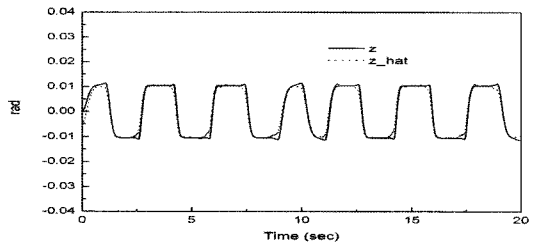

Fig. 13 Simulated results of the SOB+RFNR control system for the disturbed system: z and $\hat{z}$

control system are decreased in very low value due to the friction state observer. Next, for case 2, to investigate the performance of the adaptive robust estimator, the simulation for a perturbed friction system is carried out under the condition of the same controller parameters like the previous one. In Fig. 12 and 13, the estimation performance for the friction state of the SOB control system is deteriorated than that of the SOB+RFNR control system due to its lack of the adaptation property for the uncertainty. Thus, it can be known that the friction state observer without

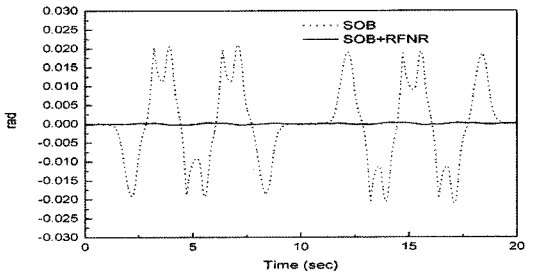

Fig. 14 Simulated results of the SOB and SOB+RFNR control system for the disturbed system: tracking errors

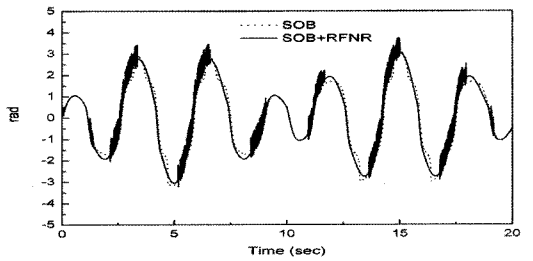

Fig. 15 Simulated results of the SOB / SOB+RFNR control system for the disturbed system: control input

containing robust term cannot cover the friction parameter variations. Therefore, the tracking error of the SOB+RFNR control system is significantly decreased comparing with the SOB control system as shown in Fig. 14 under the condition that the control input of both control system is similar as shown in Fig. 15.

3.2 Results of Experiment

The experiment results are provided to demonstrate the effectiveness of the proposed SOB+RFNR control system. The control algorithms are programmed in 'Turbo-C' language in DOS-mode and the control signals are transmitted into the DC motor drive through the DR8330 data acquisition board. The position information of the mechanical servo system is transmitted into the computer through the PCL-833 encoder counter board. The sampling rate is set to be 4ms in order to consider the calculation burden on the online training and updating parameters of the RFNN,

calculation of SOB+RFNR controller, calculation of the friction state observer and adaptive error estimator.

In the experiment, to investigate the effectiveness the proposed control system, three control schemes are designed like the previous simulations SMC, SOB, and SOB+RFNR control system. The command input is chosen by $q_d = 0.2 \times \exp(2\pi \times 0.3t) \times \sin(2\pi \times 0.05t)$. The RFNN has also two, five, five, and one neuron at the input, membership, rule and output layers, respectively. The common controller's parameters such as c_1, c_2 and β are set to be same values in each control system. The friction parameters of the SOB and SOB+RFNR controller are also set to be same values. The command input and obtained position and control input of the SMC control system are shown in Fig. 16-17. The position tracking performance of the SMC control system is very poor like simulation. If we increase the controller's gains of the SMC to improve the tracking performance, the chattering due to the friction dynamics will be greatly increased, and it causes the wear of the motor. Also the stability of the entire control system can be worsened and the actuator saturation or uncontrollable dangerous situation that often appears in feedback control system is possible to be occurred. Since this trial is not desirable to real implementations, it can be concluded that the SMC control system without friction observer is not appropriate to be used to control the precise friction dynamics. In case of the SOB and SOB+RFNR control system, the tracking errors are greatly decreased by virtue of the friction state observer like the results in simulation as shown in Fig. 18-21. The control inputs take the appropriate values though small chatterings in

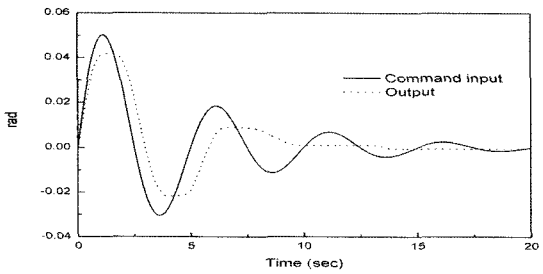

Fig. 16 Experimental results of the SMC control system: tracking performance

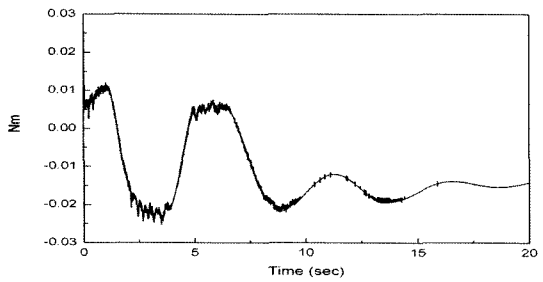

Fig. 17 Experimental results of the SMC control system: control input

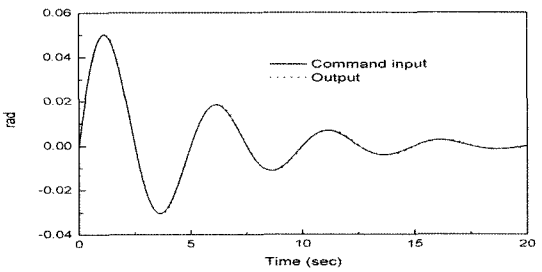

Fig. 18 Experimental results of the SOB control system: tracking performance

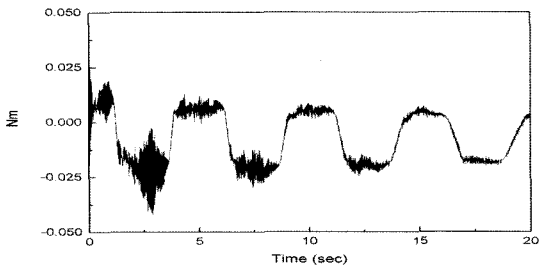

Fig. 19 Experimental results of the SOB control system: control input

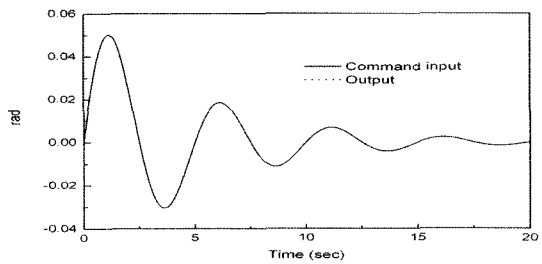

Fig. 20 Experimental results of the SOB+RFNR control

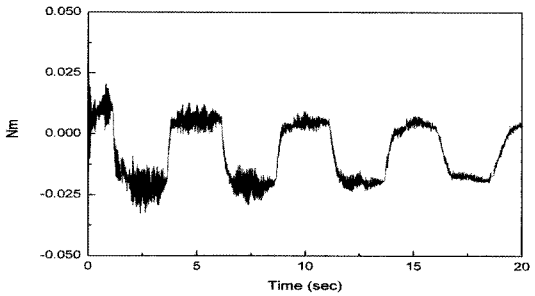

Fig. 21 Experimental results of the SOB+RFNR control system: control input

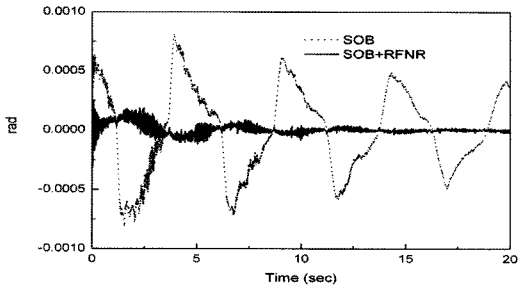

Fig. 22 Tracking errors of the SOB and SOB+RFNR control system

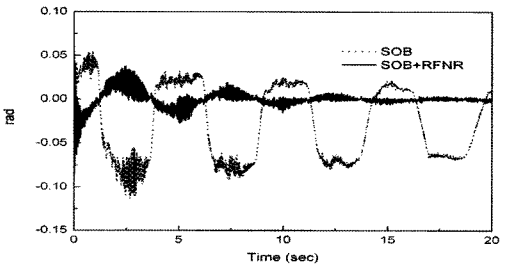

Fig. 23 Estimation of the friction state z of the SOB and SOB+RFNR control system

the turning direction of ball-screw appear in it. However, since the measured friction parameters in Table 1can be varied as operating conditions and can be different to the real values, the chosen friction parameters of each controller cannot be also said to the optimal values.

Therefore, the robust control using the RFNN estimator and adaptive approximation error estimator have to be considered. The experiment to examine the In Fig. 23, it

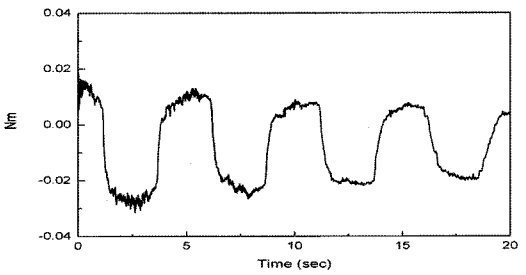

Fig. 24 Estimation of the lumped uncertainty U of the SOB+RFNR control system

is thought that the magnitude of the estimated friction state, $\hat{z}$, of the SOB+RFNR control system is small than that of the SOB control system since most of uncertainty of the friction is compensated by the uncertainty error estimator in Eq. (41). The estimated value of the lumped system uncertainty including frictional uncertainty is presented in Fig. 24, robustness to these uncertainty shows that the tracking error of the proposed SOB+RFNR control system when compared with SOB control system is greatly decreased even though the tracking error of the SOB system is small as shown in Fig. 22. Therefore, it can be known that the proposed control system is very robust to uncertainty caused by the variations of the friction parameter. Even though the friction state observer can estimate the immeasurable friction state of the mechanical servo very well in nominal case, it cannot treat efficiently the variations of the friction parameter, which is similar to the pattern of the control input shown in Fig. 21. Therefore, it is concluded that the adaptive error estimator must be necessarily considered in order to obtain more precise position tracking performance in low velocity range.

4. Conclusions

In this paper, the adaptive robust sliding mode control using RFNN and uncertainty estimator is proposed to estimate the unknown friction state and variations of the friction parameter of the mechanical servo system for the precise position tracking performance. First, the friction state observer is designed to estimate unknown state of

the LuGre dynamic friction model. Next, to estimate the variations of the friction parameters, the online RFNN algorithm combined with sliding mode control is also designed to compensate the friction uncertainty. Finally, the adaptive error estimator is designed for the estimation error caused by the approximation by the RFNN. Some simulated and experimental results for the mechanical servo system are provided to demonstrate the effectiveness of the proposed control scheme. It is shown that the proposed control scheme guarantees the robustness to the frictional uncertainty and the precise position tracking performance in micro mechanical system.

It is expected that the proposed control scheme of this paper will be very usefully applied to the micro contacted mechanical system such as electrical mechanical actuators, which are recently often reported in researches of the precise actuator systems.

References

(1) Canudas de Wit, C., Olsson, H., and Astrom, K. J., 1995, "A New Model for Control of Systems with Friction," *IEEE Trans. Automat. Contr.*, Vol. 40, No. 3, pp. 419~425.

(2) Dupong, P., Hayward, V., Armstrong, B., and Altpeter, J., 2002, "Single State Elasto-plastic Friction Models," *IEEE Trans. Automat. Contr.*, Vol. 47, No. 5, pp. 787~792.

(3) Swevers, J., Al-Bender, F., Ganseman, C., and Prajogo, T., 2000, "An Integrated Friction Model Structure with Improved Structure with Improved Presliding Behavior for Accurate Friction Model Structure," *IEEE Trans. Automat. Contr.*, Vol. 45, No. 4, pp. 675~686.

(4) Al-Bender, F., Lampaert, V., and Swever, J., 2005, "The Generalized Maxwell-slip Model: A Novel Model for Friction Simulation and Compensation," *IEEE Trans. Automat. Contr.*, Vol. 50, No. 11, pp. 1883~1887.

(5) Choi, J. J., Han, S. I., and Kim, J. S., 2006, "Development of a Novel Dynamic Friction Model and Precise Tracking Control Using Adaptive Back-stepping Sliding Mode Controller," *Mechatronics*, Vol. 16, pp. 97~104.

(6) Mayergoyz, I. D., 1991, *Mathematical Models of Hysteresis*, Springer-verlag, New York.

(7) Deur, J., 2001, "Modeling and Analysis of Longitudinal Tire Dynamics Based on the Lugre Friction Model," *In Proc. 12th IFAC World Con. AC*, Vol. 1, pp. 15~22.

(8) Alvarez, L., Yi, J. G., Horowitz, R., and Olmos, L., 2005, "Dynamic Friction Model-based Tire-road Friction Estimation and Emergency Braking Control," *Trans. ASME*, Vol. 127, March, pp. 22~32.

(9) Li, L., Wang, F. Y., and Zhou, Q. Z., 2006, "Integrated Longitudinal and Lateral Tire/road Friction Modeling and Monitering for Vehicle Motion Control," *IEEE Trans. Intell. Transp. Sys.*, Vol. 7, No. 1, pp. 1~17.

(10) Selmic, R. R. and Lewis, F. L., 2002, "Neural-network Approximation of Piecewise Continuous Functions: Application to Friction Compensation," *IEEE Trans. Neural Nets.*, Vol. 13, No. 3, pp. 745~751.

(11) Ha, Q. P., Rye, D. C., and Durrent-Whyte, H. F., 2000, "Variable Structure Systems Approach to Friction Estimation and Compensation," *Proc. IEEE Inter. Confr. On Robot & Auto.*, pp. 3543~3548.

(12) Iwasaki, M., Shibata, T., and Matui, N., 1999, "Disturbance Observer Based Nonlinear Friction Compensation in Table Drive System," *IEEE/ASME on Mechatr.*, Vol. 4, No. 1, pp. 3~8.

(13) Han, S. I., 2002, "The Position Tracking Control of Precise Servo Systems with Nonlinear Dynamic Friction Using Variable Structure Control and Friction Observer," *Inter. Journ. of JSME Series C*, Vol. 45, No. 3, pp. 784~793.

(14) Lin, C. T. and Lee, C. S. G., 1996, *Neural Systems: A Neural-fuzzy Synergism to Intelligent System*, Prenctice-Hall, International edition.

(15) Leu, Y. G., Lee, T. T., and Wang, W. Y., 1997, "On-line Tuning of Fuzzy-neural Networks for Adaptive Control of Nonlinear Dynamic Systems," *IEEE Trans. System Man Cybern.*, Vol. 27, No. 6, pp. 1034~1043.

(16) Lin, F. J., Hwang, W. J., and Wai, R. J., 1997, "A

Supervisory Fuzzy Neural Network Control System for Tracking Periodic Inputs," *IEEE Trans. Fuzzy Syst.*, Vol. 7, No. 1, pp. 41~52.

(17) Wai, R. J. and Lin, F. J., 1999, "Fuzzy Neural Network Sliding-mode Position Controller for Induction Servo Motor Drive," *IEE Proc. Electr. Power Appl.*, Vol. 146, No. 3, pp. 297~308.

(18) Lin, F. J. and Wai, R. J., 2003, "Robust Recurrent Fuzzy Neural Network Control for Linear Synchronous Motor Drive System," *Neurocomputing*, Vol. 50, pp. 365~390.

(19) Lin C. H., 2004, "Adaptive Recurrent Fuzzy Neural Network Control for Synchronous Reluctance Motor Servo Drive," *IEE Proc Electr. Power Appl.*, Vol. 151, No. 6, pp. 711~724.

(20) Peng, J. Z., Wang, Y. N., and Sun, W., 2007, "Trajectory-tracking Control for Mobile Robot Using Recurrent Fuzzy Cerebellar Model Articulation Controller," *Neural Inform Process-Letters & Rev.*, Vol. 11, No. 1, pp. 15~23.

(21) Slotine, J. E. and Li, W., 1991, *Applied Nonlinear Control*. Prentice-Hall.